16th World Congress in Computational Mechanics (WCCM)
21-26 July 2024, Vancouver, Canada
A. Korobenko, M. Laforest, S. Prudhomme, R. Vaziri (Eds)

FINITE ELEMENT-BASED SIMULATION OF LARGE WIND TURBINES WAKE USING THE ACTUATOR LINE METHOD

Vincenzo Morici*[1], Valerio Francesco Barnabei[1], Alessio Castorrini[1], Franco Rispoli[1] and Artem Korobenko[2]

[1] Sapienza University of Rome
vincenzo.morici@uniroma1.it

[2] University of Calgary
artem.korobenko@ucalgary.ca

Key words: Wind turbine, Stabilized FEM, RBVMS, Actuator Line Method.

Abstract. The numerical simulation of wind turbines and wind farms aerodynamics represents an open challenge in computational mechanics. It involves multi-physics and multi-scale phenomena, turbulent flows at very large Reynolds numbers, atmospheric boundary layer features, and rotor machinery flow features and dynamics. The geometrically resolved Computational Fluid Dynamics (CFD) is recognized as the highest-fidelity approach for wind turbine simulations but it has still a too high computational cost if employed for wind farm flow analysis. For this application, several reduced-order models have been formulated to obtain reliable results at a sustainable computational effort. Among the others, Large Eddy Simulations (LES) with Actuator Line Model (ALM) represents a valid middle-fidelity alternative for accurately simulating the wind turbine wakes dynamics and its interaction with the atmospheric boundary layer turbulence. Most implementations of the ALM are derived for volume-based CFD solvers. In this work we present the implementation of this model in a Finite Element Method (FEM) framework, which allows the use of a Residual Based Variational Multiscale (RBVMS) method to model the turbulent flow field, instead of the standard LES formulation. The ALM-VMS formulation is applied to study a 5MW and a 15MW wind turbine rotors, comparing the results with data available in literature in terms of aerodynamic variables of main interest, such as rotor loads and aerodynamics and near and far wake features.

1 INTRODUCTION

In recent decades, wind technology has emerged as a key component in the global strategy for transitioning to green energy [1, 2]. The constantly increasing dimensions of the wind turbines (WT) has made clear the need of highly reliable simulation tools to compensate the technological and economical impossibility of testing machines of radius higher than 120m [3] and wind farms of several kilometres of extension. Therefore, numerical simulations play a crucial role in validating new technological solutions and accurately assessing loads and aero-

dynamic losses (such as wake losses). This capability is essential for optimizing the design and operation and maintenance (O&M) of power plants, ultimately reducing associated costs.

One of the primary challenges in this field is the aerodynamic simulation of WT and wind farm flows. Geometrically resolved CFD [4, 5] currently offers the highest fidelity in simulations but comes with significant computational costs. Instead, the simulation tools commonly adopted in industrial applications are based on the Blade Element Momentum (BEM) theory [6], a low-fidelity approach that, through enhancement and correction modelling [7, 8], is used in the implementation of very fast tools for aero-servo-elastic simulations of the wind turbines. While this method provides quick estimates of WT dynamics, it lacks accuracy in off-design conditions and does not address wake and WTs interactions. Higher-order models, such as the Vortex Lattice Model (VLM) [9], Vortex Particle Method (VPM) [10], or panel methods [11], can resolve wake interactions but cannot model neither the entire wind farm flow in complex domains nor the Atmospheric Boundary Layer (ABL).

It is then clear how the optimal method would be a compromise between the high-fidelity fully resolved CFD and the high-efficiency BEM. For this reason, mid-fidelity methods are rapidly gaining attention, being able to simulate the wind flow through turbulent CFD and solve all the features of the ABL [12, 13, 14]. These methods significantly reduce the computational costs associated with simulating the wind turbine rotor. Notable among these are the Actuator Disk Method (ADM) [15] and the Actuator Line Method (ALM) [16, 17].

Most implementations of the ALM are derived for finite volume CFD solver (Sørensen, 1995; Michelsen, 1992), with the most used opensource library of ALM for finite volume CFD (SOWFA [18] and turbinesFoam [19]) based on LES. Korobenko et al. [20] demonstrated the potential of using the ALM in the framework of finite element and Isogeometric Analysis (IGA) [21], obtaining highly accurate description of the atmospheric turbulence for different class of ABL stability with the RBVMS method, which have been validated and applied successufully on a large range of fluid mechanics applications [22, 23, 24, 25].

This work presents the results of implementing the Actuator Line Model in the FEM-based framework developed by the authors [26, 27, 28, 29, 30], with the novel application to large-scale wind turbines. The potential of using the VMS model for solving the turbulent flow field generated by the rotor and wake is verified by comparing the performance of two different wind turbines with the available literature. A first case focuses on the IEA Wind 15MW reference wind turbine [3], comparing the results with those of another authors' work [31] on the same turbine. A second case focuses on the NREL 5MW reference wind turbine [32], comparing the results with those of Troldborg et al. [33] and focusing in particular on the capability of the solver of properly deriving the wake dynamics both in the near and far wake. Both cases will have as reference results from geometry-resolved CFD simulations, for a correct assessment of the performance of this novel ALM-VMS implementation.

A general overview of the methodology used to conduct the analysis will be provided in Section 2. Section 3 will then describe the two different test cases used in this work and the results of these analysis will be discussed in Section 4.

2 METHODOLOGY

2.1 COMPUTATIONAL FLUID DYNAMICS MODEL

Let $\Omega_1 \subset I\!R^{n_{sd}}$ be the spatial domain of the fluid, with boundary defined by Γ_1. The Navier–Stokes equations of incompressible flows can be written on Ω_1 and $\forall t \in (0, T)$ as

$$\rho\left(\frac{\partial \mathbf{u}}{\partial t} + \mathbf{u}\cdot\boldsymbol{\nabla}\mathbf{u} - \mathbf{f}\right) - \boldsymbol{\nabla}\cdot\boldsymbol{\sigma}_1 = \mathbf{0}, \tag{1}$$

$$\boldsymbol{\nabla}\cdot\mathbf{u} = 0, \tag{2}$$

where ρ is the density, $\mathbf{u}$ the velocity, $\mathbf{f}$ the body force, and the stress tensor is defined as $\boldsymbol{\sigma}_1(p,\mathbf{u}) = -p\mathbf{I} + \mu\boldsymbol{\varepsilon}(\mathbf{u})$. Here, p and μ are the pressure and the viscosity, $\mathbf{I}$ is the identity tensor, and $\boldsymbol{\varepsilon}(\mathbf{u}) = \frac{1}{2}\left((\boldsymbol{\nabla}\mathbf{u}) + (\boldsymbol{\nabla}\mathbf{u})^T\right)$ is the strain-rate tensor.

We assume then finite-dimensional trial solution and test function spaces for the coarse scale fluid velocity and pressure, respectively defined as $\mathbf{u}^h$, p^h, and $\mathbf{w}_1^h$, q_1^h, where the superscript "h" indicates that the finite-dimensionality of the function.

The RBVMS formulation of the Navier-Stokes equations in Ω_1 used in the present case study is derived according to [22, 23, 34, 35, 28] as follows:

$$\begin{aligned}
&\int_{\Omega_1} \mathbf{w}_1^h\cdot\rho\left(\frac{\partial \mathbf{u}^h}{\partial t} + \mathbf{u}^h\cdot\boldsymbol{\nabla}\mathbf{u}^h - \mathbf{f}\right)\mathrm{d}\Omega + \int_{\Omega_1}\boldsymbol{\varepsilon}(\mathbf{w}_1^h):\boldsymbol{\sigma}_1^h\mathrm{d}\Omega \\
&\quad+\int_{\Omega_1} q_1^h\boldsymbol{\nabla}\cdot\mathbf{u}^h\mathrm{d}\Omega \\
&\quad+\sum_{e=1}^{n_{el}}\int_{\Omega_1^e}\frac{\tau_{\mathrm{SUPS}}}{\rho}\left(\rho\mathbf{u}^h\cdot\boldsymbol{\nabla}\mathbf{w}_1^h + \boldsymbol{\nabla}q_1^h\right)\cdot\mathbf{r}_{\mathbf{M}}\mathrm{d}\Omega \\
&\quad+\sum_{e=1}^{n_{el}}\int_{\Omega_1^e}\nu_{\mathrm{LSIC}}\boldsymbol{\nabla}\cdot\mathbf{w}_1^h\rho\mathrm{r}_{\mathrm{C}}\mathrm{d}\Omega \\
&\quad-\sum_{e=1}^{n_{el}}\int_{\Omega_1^e}\tau_{\mathrm{SUPS}}\mathbf{w}_1^h\cdot\left(\mathbf{r}_{\mathbf{M}}\cdot\boldsymbol{\nabla}\mathbf{u}^h\right)\mathrm{d}\Omega \\
&\quad-\sum_{e=1}^{n_{el}}\int_{\Omega_1^e}\frac{\tau_{\mathrm{SUPS}}^2}{\rho}\mathbf{r}_{\mathbf{M}}\cdot\left(\boldsymbol{\nabla}\mathbf{w}_1^h\right)\cdot\mathbf{r}_{\mathbf{M}}\mathrm{d}\Omega = 0,
\end{aligned}$$

where

$$\mathbf{r}_{\mathbf{M}} = \rho\left(\frac{\partial \mathbf{u}^h}{\partial t} + \mathbf{u}^h\cdot\boldsymbol{\nabla}\mathbf{u}^h - \mathbf{f}\right) - \boldsymbol{\nabla}\cdot\boldsymbol{\sigma}_1^h, \tag{3}$$

$$\mathrm{r}_{\mathrm{C}} = \boldsymbol{\nabla}\cdot\mathbf{u}^h \tag{4}$$

are the residuals of the momentum and continuity equations. The superscript "e" is the element counter, n_{el} is the number of elements, and τ_{SUPS} and ν_{LSIC} are the stabilization parameters, for which we use the expression given in [36].

2.2 ACTUATOR LINE MODEL

The aerodynamic model of the turbine rotor blades follows that of a standard ALM [16], using the convention of [37] to define a generic blade section. In this aerodynamic model, the blade is discretized into actuator line elements, and its effect on the flow-field is represented by substituting the 3D blade geometry with a momentum source field added to the body force term $\mathbf{f}$ within the Navier-Stokes equations. Mean cross-sectional geometric and aerodynamic properties of the blade are defined for each element. A research algorithm is used to locate the center of each element within a fluid volume element, where the velocity is interpolated using the FEM shape functions. This velocity, along with tabulated aerodynamic coefficients, is then used to calculate the total aerodynamic force at the centroid. The force are then distributed onto the fluid domain using a three-dimensional kernel function, expressed as

$$\mathbf{f}_{\varepsilon} = \mathbf{f} \otimes \eta_{\varepsilon} \,, \tag{5}$$

where

$$\eta_{\varepsilon}(r) = \frac{1}{\varepsilon^3 \pi^{3/2}} exp\left[- \left(\frac{r}{\varepsilon} \right)^2 \right] . \tag{6}$$

Here r is the distance between the center of the actuator element under consideration, origin of the force source, and the measuring point, and ε is a constant that defines the strength of the regularization function. In this work the chosen strategy for computing ε is the one proposed by Troldborg et al [38], which indicates that a good approximation of ε would be at least twice the local grid cell length.

Also, Martinez et al. reports in [39] that one of the main requirements of the ALM is that $\Delta b / \Delta x < 0.75$, where Δb is the average blade element length and Δx is the most refined cell dimension in the rotor zone of the computational domain.

A loss correction based on the lifting line theory is applied to the lift coefficient used in the element force computation, to account for end effects of the finite blade at both root and tip. It's implementation follows the one reported in [40].

3 CASE STUDY

3.1 Wind turbines

The two turbines chosen for this study are the IEA Wind 15MW [3] and the NREL 5MW [32] reference wind turbines.

The 15MW horizontal axis wind turbine (HAWT) features $117\,\mathrm{m}$ long blades, constrained to the rotor hub at a distance of $3.97\,\mathrm{m}$ from the rotor axis, for a resulting rotor diameter of $242\,\mathrm{m}$. For this turbine, a coning angle of $4\,\mathrm{deg}$ is used, which, considering the blade tip prebend of $4\,\mathrm{m}$, leads to an upstream tip deflection of $12\,\mathrm{m}$. Since no tower is considered in this case study, the rotor is centered in the computational domain.
The aerodynamic properties of the turbine blades are defined for 50 uniformly-spaced airfoil sections along the blade span, giving actuator elements of $2.387\,\mathrm{m}$. With a rotor cell dimension

of $5\,\mathrm{m}$ for the adopted mesh resolution, this discretization respects the requirement presented in 2.2 with a final ratio of $\Delta b/\Delta x = 0.477$.

The 5MW HAWT features $61.5\,\mathrm{m}$ long blades, constrained to the rotor hub at a distance of $1.5\,\mathrm{m}$ from the rotor axis. With no coning angle for this case study, the resulting rotor diameter is $126\,\mathrm{m}$. The rotor is mounted at an height of $90\,\mathrm{m}$ from the ground, to reproduce the reference literature configuration. No tower is considered in this case study.
The aerodynamic properties of the turbine blades are defined for 62 uniformly-spaced airfoil sections along the blade span, giving actuator elements of $1.008\,\mathrm{m}$. Given a rotor cell dimension of $3.34\,\mathrm{m}$ for the adopted mesh resolution, the final ratio between actuator elements and local cell dimension is $\Delta b/\Delta x = 0.3$.

3.2 Computational domain and numerical setup

The computational domain for the 15MW case study consists of a cubic box of side length $10\,\mathrm{D}$, with the rotor centered in the domain. The mesh, shown in Figure 1, is a hexahedral mesh containing 1.15 M 8-nodes hexahedron finite elements. A refinement is applied in the rotor zone, extending $1.2\,\mathrm{D}$ in both Y and Z directions, and extending $40\,\mathrm{m}$ upstream and $1\,\mathrm{D}$ downstream of the rotor, to obtain a minimum element dimension of $5\,\mathrm{m}$.

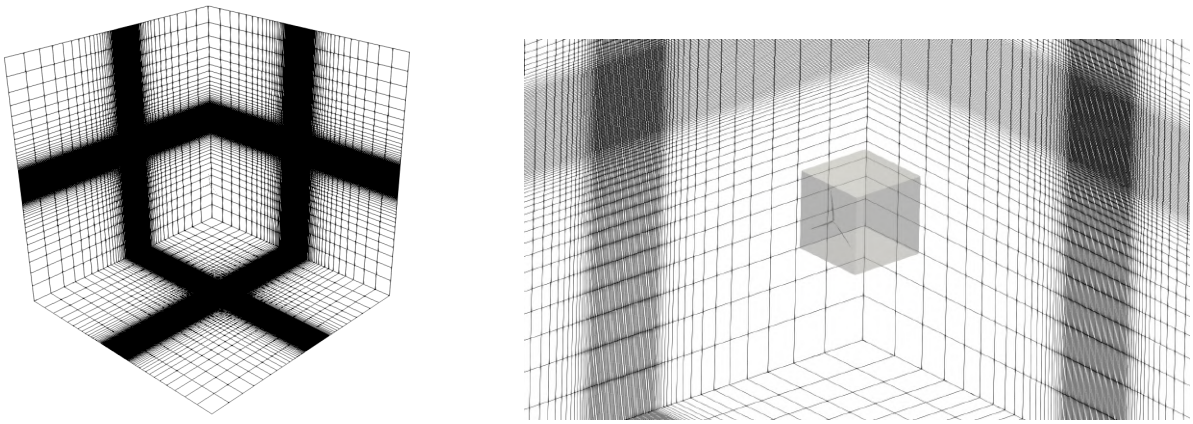

(a) (b)

Figure 1: Computational domain for the 15MW case study, a) general view and b) detail of refinement.

The computational domain for the 5MW case study is the same as defined in [33]. The domain extends $8\,\mathrm{D}$ upstream and $12\,\mathrm{D}$ downstream of the turbine, which is located $90\,\mathrm{m}$ above the level of the ground, and has the shape of a half-cylinder of radius $8\,\mathrm{D}$. The mesh, shown in Figure 2, is a hexahedral mesh containing 2.7 M cells. A refinement is applied in the rotor zone, extending $1.5\,\mathrm{D}$ both in Y and Z direction, to obtain a $3.34\,\mathrm{m}$ fluid element dimension. This refinement is then extended $1\,\mathrm{D}$ upstream and $7\,\mathrm{D}$ downstream of the turbine, with the elements gradually increasing in dimension towards the far field.

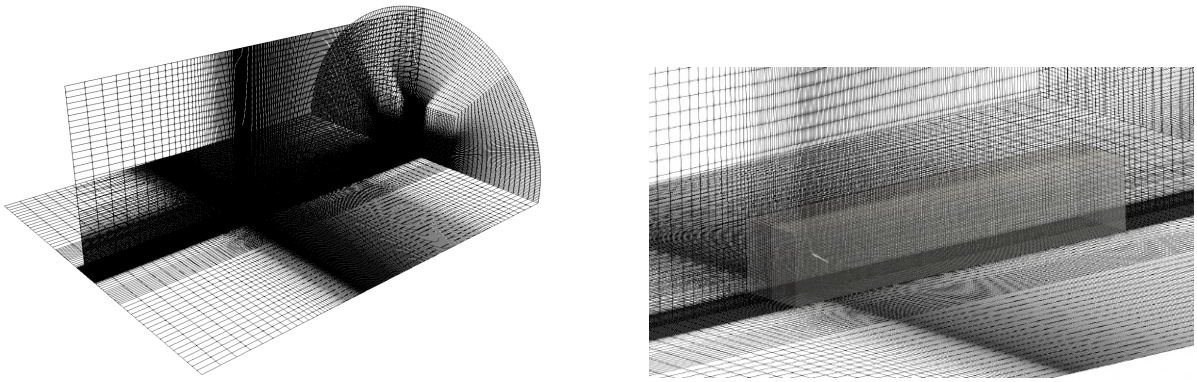

(a) (b)

Figure 2: Computational domain for the 5MW case study, a) general view and b) detail of refinement.

Both the study cases have uniform inflow conditions at the inlet patch, with an inflow velocity of $7.5\,\mathrm{m/s}$ for the 15MW rotor and $8\,\mathrm{m/s}$ for the 5MW rotor, while a slip condition is applied to all the other boundary patches. They both have run for $500\,\mathrm{s}$ of physical time, with the time-averaged flow field quantities computed from $350\,\mathrm{s}$ for the 15MW case and from $250\,\mathrm{s}$ until the end for the 5MW case. For the 15MW case the timestep size is $0.05\,\mathrm{s}$, while it is $0.025\,\mathrm{s}$ for the 5MW case, with the coupled non-linear system of equations solved using three iterations of Newton-Rhapson for each timestep.

4 RESULTS

The analysis of the results is presented for the two separate cases, focusing on the turbine performance in the 15MW case and on the wake dynamics in the 5MW case.

4.1 15MW case study results

The analysis of the performance of the 15MW turbine rotor are presented in terms of aerodynamic loads and angle of attack along the blade span. These results, shown in Figures 3 and 4, are compared to those of [31], focusing in particular on the comparison with results obtained using the ALM implemented in OpenFOAM [19] and run within a Detached Eddy Simulation (DES), a geometry resolved Reynolds Averaged Navier Stokes (RANS) simulation of a single-blade periodic sector, and a BEMT-based solver (*Aerodyn v.15* [41]).

Figure 3 shows a very close match of the normal force distribution with the other ALM code, with the same loss of aerodynamic load towards the tip. The tangential force distribution shows a slight under prediction of the load in the central part of the blade with respect to the geometry resolved data, while behaving very similarly to the BEMT model.

Figure 4 shows the geometric angle of attack distribution along the blade span. ALM and BEMT codes show an under prediction of the values in the first third of the blade span with respect to the geometry resolved case, while the results are very similar for the most loaded

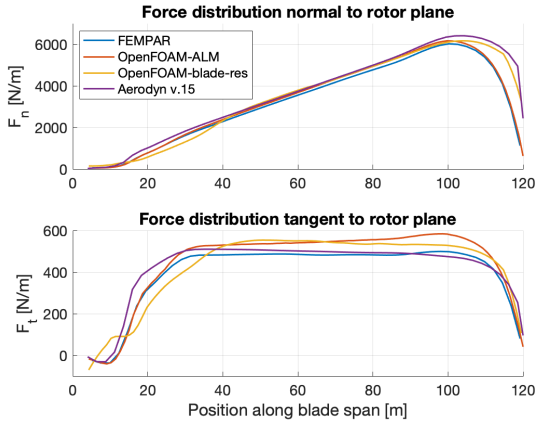

Figure 3: Normal (top) and tangential (bottom) aerodynamic force distribution over the 15MW blade, averaged over the last rotor revolution [31].

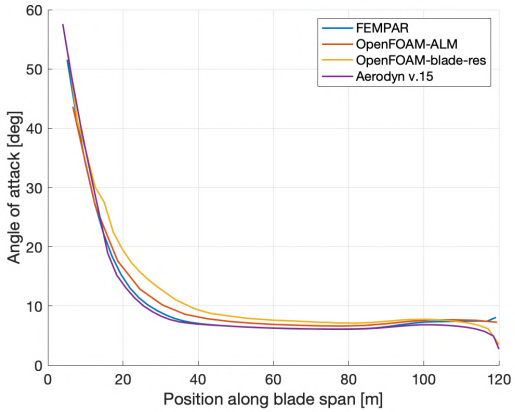

Figure 4: Geometric angle of attack distribution over the 15MW blade, averaged over the last rotor revolution [31].

portion of the blade.

4.2 5MW case study results

This section will focus on a comparison of the wake statistics with the results obtained by Troldborg et al. [33]. Figure 5 offers a plot of the vorticity magnitude in a meridian plane of the domain, passing through the rotor center. The wake structure keeps ordered until 5D after which the turbulent wake starts to mix with the undisturbed flow field. A Q-criterion contour is shown in Figure 6 showing the development of stable tip vortex structures in the near wake. The velocity deficit and the turbulent kinetic energy in the wake are plotted in Figures 7 and 8, respectively. Figure 7 shows how the current ALM implementation gives a velocity deficit in the turbine wake that closely resembles that of the ALM-ADM of the reference. In particular, in the middle part of the blade the deficit appears slightly overestimated, while towards root and tip two different phenomena are worth mentioning. First, as the distance from the rotor increases, the tip velocity deficit become lower than the reference. Second, the velocity profile

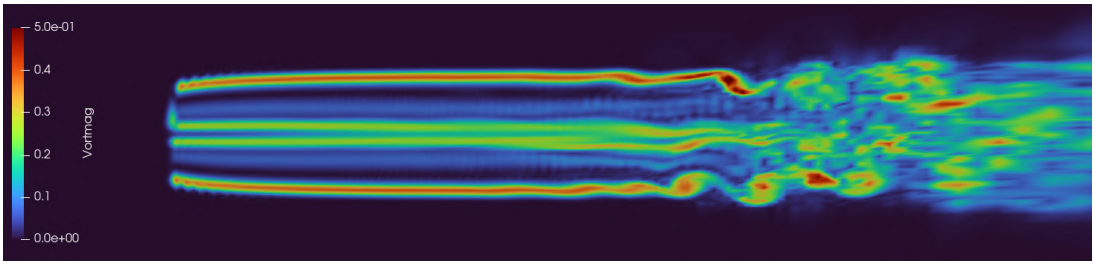

Figure 5: Vorticity magnitude in the wake of the 5MW rotor (top view).

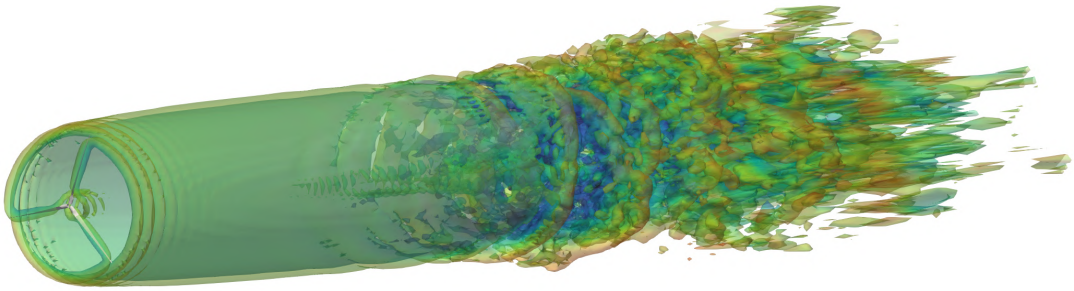

Figure 6: Q-criterion contour ($Q = 0.035$).

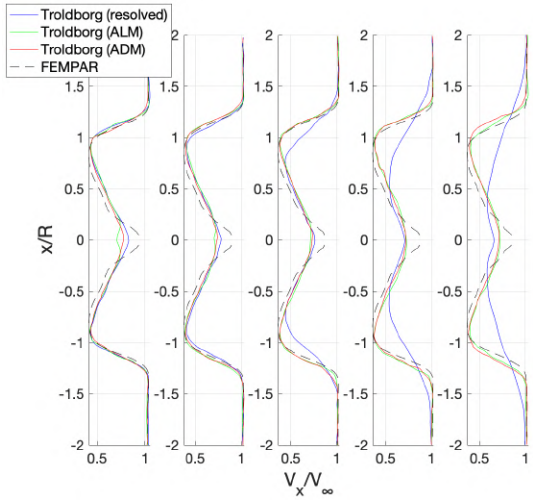

Figure 7: Stream-wise velocity deficit in the wake of the 5MW turbine rotor [33].

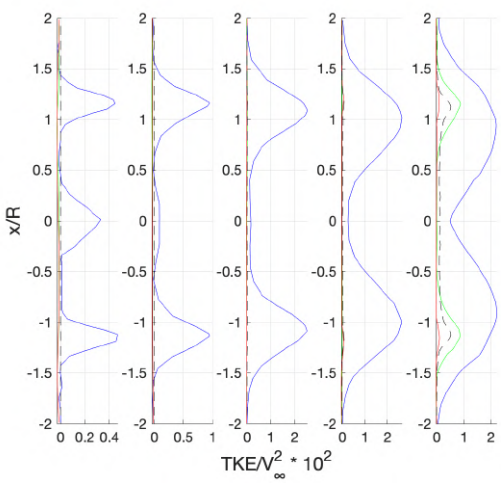

Figure 8: Turbulent kinetic energy in the wake of the 5MW turbine rotor [33].

in the middle of the rotor suggests that either a better end effect for the blade root or the presence of the hub should be considered to better match the reference data.

The turbulent kinetic energy profiles in Figure 8 gives similar results to the ALM-ADM implementations of the reference, confirming a very low turbulence production in the wake behind a rotor modelled using these techniques.

5 CONCLUSIONS

This study presented an investigation on the use of an Actuator Line Model in a FEM-based tool for wind turbine performance assessment. The theory underlying the problem has been described in the second section and a brief focus on the turbine modelling process has been done in the third section. Two different test cases were chosen for the study, to demonstrate the validity of the predictions of the tool with respect to reference literature.

The 15MW rotor test case demonstrated the capabilities of the tool of correctly predicting

the rotor performance. Although only few aerodynamic results have been taken into consideration, they showed errors within acceptable ranges, as demonstrated by the reference literature. They also suggested the use of a better end effect model for the ALM, to properly catch the aerodynamics towards the blade tip.

The 5MW rotor test case focused instead on demonstrating the capabilities of the tool of assessing the main aerodynamics characteristics in the wake dynamics. The comparison with the reference literature showed a dynamic development of the wake in line with the prediction of similar codes, but underlined the necessity of taking into consideration a better end effect for the blade root or the presence of the rotor hub, to reduce the error in the rotor center.

6 ACKNOWLEDGMENTS

The project was partially supported by the Ministry of Enterprises and Made in Italy under Grant Agreement "RdS PTR 2022-2024 - Energia elettrica dal mare", and by the Italian Ministry of University and Research (MUR) as part of the EU programme NextGenerationEU, PNRR - M4C2 - PE0000021 "NEST - Network 4 Energy Sustainable Transition" in Spoke 2 "Energy Harvesting and offshore renewables".

References

[1] P. M. Buchheit M., Vandendriessche T., "A european strategy of offshore renewable energy," 2022.

[2] E. Commission, D.-G. for Energy, S. K., K. I., and e. a. Ramaekers L., "Study on the offshore grid potential in the mediterranean region: final report," 2020.

[3] G. Evan, J. Rinker, L. Sethuraman, F. Zahle, B. Anderson, G. Barter, N. Abbas, F. Meng, P. Bortolotti, W. Skrzypinski, G. Scott, R. Feil, H. Bredmose, K. Dykes, M. Shields, C. Allen, and A. Viselli, "Definition of the iea 15-megawatt offshore reference wind turbine," tech. rep., International Energy Agency, 2020.

[4] S. Kalvig, E. Manger, and B. Hjertager, "Comparing different cfd wind turbine modelling approaches with wind tunnel measurements," *Journal of Physics: Conference Series*, 2014.

[5] A. Korobenko, M.-C. Hsu, I. Akkerman, J. Tippmann, and Y. Bazilevs, "Structural mechanics modeling and fsi simulation of wind turbines," *Mathematical Models and Methods in Applied Sciences*, vol. 23, pp. 249–272, 02 2013.

[6] H. Glauert, "Airplane propellers," *Springer Berlin Heidelberg*, 1935.

[7] H. A. Madsen, T. J. Larsen, G. R. Pirrung, A. Li, and F. Zahle, "Implementation of the blade element momentum model on a polar grid and its aeroelastic load impact," *Wind Energy Science*, vol. 5, no. 1, pp. 1–27, 2020.

[8] L. Wang, X. Liu, N. Renevier, M. Stables, and G. M. Hall, "Nonlinear aeroelastic modelling for wind turbine blades based on blade element momentum theory and geometrically exact beam theory," *Energy*, vol. 76, pp. 487–501, 2014.

[9] J.-J. Chattot, "Helicoidal vortex model for wind turbine aeroelastic simulation," *Computers and Structures*, vol. 85, no. 11, pp. 1072–1079, 2007. Fourth MIT Conference on Computational Fluid and Solid Mechanics.

[10] P. Chatelain, L. Bricteux, S. Backaert, G. Winckelmans, S. Kern, and P. Koumoutsakos, "Vortex particle-mesh methods with immersed lifting lines applied to the large eddy simulation of wind turbine wakes," 01 2011.

[11] L. Greco and C. Testa, "Wind turbine unsteady aerodynamics and performance by a free-wake panel method," *Renewable Energy*, vol. 164, pp. 444–459, 2021.

[12] M. Ravensbergen, T. Helgedagsrud, Y. Bazilevs, and A. Korobenko, "A variational multiscale framework for atmospheric turbulent flows over complex environmental terrains," *Computer Methods in Applied Mechanics and Engineering*, vol. 368, p. 113182, 2020.

[13] M. Dörenkämper, B. Witha, G. Steinfeld, D. Heinemann, and M. Kühn, "The impact of stable atmospheric boundary layers on wind-turbine wakes within offshore wind farms," *Journal of Wind Engineering and Industrial Aerodynamics*, vol. 144, pp. 146–153, 2015. Selected papers from the 6th International Symposium on Computational Wind Engineering CWE 2014.

[14] A. Castorrini, V. Morici, F. De Girolamo, L. Tieghi, V. Barnabei, and A. Corsini, "Investigation of turbines wakes and wake-rotor interaction in a floating offshore wind farm," pp. 242–249, 01 2023.

[15] M. F. Howland, J. Bossuyt, L. A. Martínez-Tossas, J. Meyers, and C. Meneveau, "Wake structure in actuator disk models of wind turbines in yaw under uniform inflow conditions," *Journal of Renewable and Sustainable Energy*, vol. 8, p. 043301, 07 2016.

[16] J. Sorensen and W. Z. Shen, "Numerical modeling of wind turbine wakes," *Journal of Fluids Engineering*, vol. 124, p. 393, 06 2002.

[17] L. Martínez Tossas, S. Leonardi, M. Churchfield, and P. Moriarty, "A comparison of actuator disk and actuator line wind turbine models and best practices for their use," 01 2012.

[18] S. L. M. Churchfield, *NWTC design codes (SOWFA)*, 2013.

[19] P. Bachant, A. Goude, daa mec, and M. Wosnik, "turbinesfoam/turbinesfoam: v0.1.1," Nov. 2019.

[20] M. Ravensbergen, A. Bayram Mohamed, and A. Korobenko, "The actuator line method for wind turbine modelling applied in a variational multiscale framework," *Computers and Fluids*, vol. 201, p. 104465, 2020.

[21] T. Hughes, J. Cottrell, and Y. Bazilevs, "Isogeometric analysis: Cad, finite elements, nurbs, exact geometry and mesh refinement," *Computer Methods in Applied Mechanics and Engineering*, vol. 194, no. 39, pp. 4135–4195, 2005.

[22] T. Hughes, "Multiscale phenomena: Green's functions, the dirichlet-to-neumann formulation, subgrid scale models, bubbles and the origins of stabilized methods," *Computer Methods in Applied Mechanics and Engineering*, vol. 127, pp. 387–401, 11 1995.

[23] Y. Bazilevs, V. Calo, J. Cottrell, T. Hughes, A. Reali, and G. Scovazzi, "Variational multiscale residual-based turbulence modeling for large eddy simulation of incompressible flows," *Computer Methods in Applied Mechanics and Engineering*, vol. 197, no. 1, pp. 173–201, 2007.

[24] Y. Bazilevs and I. Akkerman, "Large eddy simulation of turbulent taylor–couette flow using isogeometric analysis and the residual-based variational multiscale method," *Journal of Computational Physics*, vol. 229, no. 9, pp. 3402–3414, 2010.

[25] A. Korobenko, Y. Bazilevs, K. Takizawa, and T. Tezduyar, "Computer modeling of wind turbines: 1. ale-vms and st-vms aerodynamic and fsi analysis," *Archives of Computational Methods in Engineering*, 09 2018.

[26] V. F. Barnabei, A. Castorrini, A. Corsini, and F. Rispoli, "Morphing of Reversible Axial Fan Blade: A FSI-FEM Study," *Journal of Turbomachinery*, vol. 144, p. 091013, 03 2022.

[27] *Unsteady Flow Simulation of an Axial Fan for Dry Cooling in a CSP Plant Using the Variational Multiscale Method*, vol. Volume 1: Aircraft Engine; Fans and Blowers of *Turbo Expo: Power for Land, Sea, and Air*, 09 2020.

[28] A. Castorrini, V. F. Barnabei, A. Corsini, F. Rispoli, K. Takizawa, and T. E. Tezduyar, *Computational Fluid–Structure Interaction Analysis of Passive Adaptive Blades in Turbomachinery Applications*, pp. 33–58. Cham: Springer International Publishing, 2023.

[29] *Strongly Coupled Fluid-Structure Interaction Simulation of a 3D Printed Fan Rotor*, vol. Volume 1: Aircraft Engine; Fans and Blowers; Marine; Honors and Awards of *Turbo Expo: Power for Land, Sea, and Air*, 06 2019.

[30] Barnabei, Valerio Francesco, Castorrini, Alessio, Corsini, Alessandro, and Rispoli, Franco, "Fsi analysis and simulation of flexible blades in a wells turbine for wave energy conversion," *E3S Web Conf.*, vol. 197, p. 11008, 2020.

[31] L. Tieghi, V. Morici, A. Castorrini, N. Aryan, and L. Greco, "Aerodynamic characterization of the iea 15 mw reference wind turbine by code-to-code comparison," in *The Science of Making Torque from Wind (TORQUE 2024)*, 2024.

[32] J. Jonkman, S. Butterfield, W. Musial, and G. Scott, "Definition of a 5-mw reference wind turbine for offshore system development," tech. rep., NREL/TP-500-38060, Golden, CO: National Renewable Energy Laboratory, 2009.

[33] N. Troldborg, F. Zahle, P.-E. Réthoré, and N. Sørensen, "Comparison of wind turbine wake properties in non-sheared inflow predicted by different cfd rotor models," *Wind Energy*, vol. 18, 04 2014.

[34] Y. Bazilevs, K. Takizawa, and T. E. Tezduyar, *Computational Fluid–Structure Interaction: Methods and Applications*. Wiley, February 2013.

[35] T. E. Tezduyar, K. Takizawa, and Y. Bazilevs, "Fluid–structure interaction and flows with moving boundaries and interfaces," in *Encyclopedia of Computational Mechanics Second Edition* (E. Stein, R. de Borst, and T. J. R. Hughes, eds.), Part 2 Fluids, Wiley, published online, December 2017.

[36] K. Takizawa, T. Tezduyar, and T. Kuraishi, "Multiscale space-time methods for thermo-fluid analysis of a ground vehicle and its tires," *Mathematical Models and Methods in Applied Sciences*, vol. 25, pp. 2227–2255, 11 2015.

[37] T. Larsen and A. Hansen, *How 2 HAWC2, the user's manual*. No. 1597(ver. 3-1)(EN) in Denmark. Forskningscenter Risoe. Risoe-R, Risø National Laboratory, 2007.

[38] N. Troldborg, F. Zahle, P.-E. Réthoré, and N. Sorensen, "Comparison of the wake of different types of wind turbine cfd models," in *50th AIAA Aerospace Sciences Meeting including the New Horizons Forum and Aerospace Exposition*, p. 237, 2012.

[39] L. Martinez, S. Leonardi, M. Churchfield, and P. Moriarty, "A comparison of actuator disk and actuator line wind turbine models and best practices for their use," in *50th AIAA Aerospace Sciences Meeting including the New Horizons Forum and Aerospace Exposition*, p. 900, 2012.

[40] P. Bachant, A. Goude, and M. Wosnik, "Actuator line modeling of vertical-axis turbines," 2018.

[41] P. Moriarty and A. C. Hansen, "Aerodyn theory manual," 2005.